

# Solution study of chiral 1,2-diol Yb<sup>3+</sup> chelates through near-IR circular dichroism

Moreno Lelli,<sup>a,b,†</sup> Lorenzo Di Bari<sup>a</sup> and Piero Salvadori<sup>a,\*</sup>

<sup>a</sup>*Dipartimento di Chimica e Chimica Industriale, Università di Pisa, Via Risorgimento 35, I-56126 Pisa, Italy*

<sup>b</sup>*Scuola Normale Superiore, Piazza dei Cavalieri 7, I-56126 Pisa, Italy*

Received 26 September 2007; accepted 13 November 2007

**Abstract**—Ytterbium is efficiently chelated by 1,2-diols in a variety of very different solvents. We found a set of solution equilibria among three complexes of minimum formula [Yb(diol)], [Yb(diol)<sub>2</sub>] and [Yb(diol)<sub>3</sub>]. By extensive near-Infrared circular dichroism (NIR CD) investigation, we determined fingerprint CD spectra of the di- and tri-chelated species and the relative formation constants. Since NIR CD is sensitive only to chiral Yb-species, NIR CD can be very useful for studying complex mixtures, such as those used in enantioselective catalysis and involving a chiral non-racemic diol as an auxiliary and an ytterbium salt. The chiroptical spectra show completely conserved features through very different diol structures, demonstrating the identity of the coordination polyhedron around Yb(III) and giving rise to a new empirical method for assigning 1,2-diols absolute configuration.

© 2007 Elsevier Ltd. All rights reserved.

## 1. Introduction

Chiral non-racemic diols are ubiquitous in natural compounds and can be efficiently synthesized by means of enantioselective olefin dihydroxylation.<sup>1,2</sup> They have found wide application in synthetic organic chemistry as powerful and versatile chiral auxiliaries for stereoselective reactions. Very notably their lanthanide chelates were recently demonstrated to be promising catalytic precursors in the asymmetric aldol-Tishchenko reaction.<sup>3</sup>

A promising and developing area of lanthanide chemistry has arisen in the context of molecular recognition and chirality sensing.<sup>4</sup> This is due to a dynamic coordination sphere, which allows fast exchange involving (chiral) organic ligands, and leads to the formation of the most thermodynamically stable product. The electronic structure of lanthanide ions allows us to monitor these dynamic processes spectroscopically and to use this as a probe for ligand chirality.

Following our interest in the near IR (NIR) chiroptical properties of ytterbium as the lanthanide, we have recently examined the case of a stable chelate, Yb(fod)<sub>3</sub>, where the bidentate ligand gives rise to mirror image  $\Delta/\Lambda$  pseudo-antiprismatic coordination.<sup>5</sup> In the presence of a non-racemic chiral diol, we observed a CD feature around 300 nm, allied to the  $\pi\text{--}\pi^*$  transition of the diketonate,<sup>6–8</sup> which is due to the axial binding of the diol and the consequent prevalence of one of the two  $\Delta$  or  $\Lambda$  coordination forms, which in this context are diastereomeric. We explored the scope of the correlation between absolute configuration of the diol and sign of the CD, and extended the observation window from the classical UV region to NIR.<sup>5</sup>

The good NIR CD correlation prompted us to extend our investigation to ytterbium salts, which are to some extent dissociated in polar media and where the chromophore is solely the lanthanide itself: we herein report a comprehensive investigation of the adducts arising in solution between Yb(III) ion (as the solution of Yb(OTf)<sub>3</sub> or YbCl<sub>3</sub>) and a wide range of chiral diols. We illustrate the conditions promoting the formation of these adducts and set up the spectroscopic tools allowing their prompt characterization. These findings will be useful for the rationalization of the catalytic behaviour of chiral lanthanide adducts. By comparing the near-IR Circular Dichroism (NIR CD) spectra of these mixtures, we provide a

\* Corresponding author. Tel.: +39 050 2219 273; fax: +39 050 2219 409; e-mail: [psalva@cci.unipi.it](mailto:psalva@cci.unipi.it)

† Present address: Magnetic Resonance Center (CERM), University of Florence, Sesto Fiorentino 50019 (FI), Italy.

novel and particularly simple method for the configurational assignment of 1,2-diols.

NIR CD arises from the chiroptical properties induced on the  $^2F_{7/2} \rightarrow ^2F_{5/2}$  transition of Yb(III) when the metal is surrounded by a dissymmetric coordination polyhedron.<sup>9</sup> The transitions are globally magnetically allowed ( $\Delta J = 1$ ) and give relatively strong Cotton Effects<sup>10</sup> centred around 980 nm, a region practically devoid from other contributions. Induced CD following interaction of Yb<sup>3+</sup> with chiral molecules,<sup>5,11–13</sup> as well as structured and strong spectra of stable dissymmetric complexes<sup>14–18</sup> has been reported. Notably, the Yb<sup>3+</sup> NIR CD spectrum is sensitive to changes in the metal coordination sphere and was successfully used to assess the ligand arrangement,<sup>16</sup> or to monitor processes such as solvent binding or ligand exchange.<sup>18</sup>

Thus, NIR CD is a suitable spectroscopy for the investigation of the ytterbium–diol adducts in solution. Since it only responds to chiral Yb-species, it allows us to monitor the diol coordination and the formation of all the chiral species, which are the focus of our interest, without interference from the free diol or metal ion. As NIR CD depends primarily on the dissymmetric coordination polyhedron of Yb<sup>3+</sup>, the comparison of the spectra recorded with several diols allows us to speculate on the structural arrangement of the diol around the metal and to extrapolate information about the diol absolute configuration.

## 2. Results

A very preliminary investigation indicated that there is a substantial equivalence in the behaviour of Yb(OTf)<sub>3</sub> and YbCl<sub>3</sub> towards diols, the most conspicuous differences being due to solubility effects. Therefore we concentrated primarily on Yb(OTf)<sub>3</sub>, which is more readily soluble in a large number of organic solvents.

The interaction between chiral non-racemic vicinal diols and Yb(TfO)<sub>3</sub> can be efficiently monitored and quantified by means of NIR CD spectroscopy. Around 980 nm, Yb(III) gives rise to a manifold of f–f transitions, characterized by a modest extinction coefficient but a comparatively very large circular dichroism, when the lanthanide ion is embedded in a dissymmetric environment.<sup>9</sup> Since ytterbium triflate is obviously achiral, any non-vanishing NIR CD witnesses the formation of a Yb/diol complex. As a starting point, we took a very simple enantiopure diol, (*R,R*)-2,3-butanediol **1**, and examined the behaviour of a solution of Yb(OTf)<sub>3</sub> and YbCl<sub>3</sub> in various solvents after the addition of the chiral ligand: Figure 1 reports the NIR CD spectra of such mixtures.

We can observe that

- in all cases, chiral Yb complexes are formed;
- the NIR CD spectra are structured and feature several distinct Cotton effects;
- the overall appearances of all the spectra are very similar, although the total amplitude depends on the solvent.

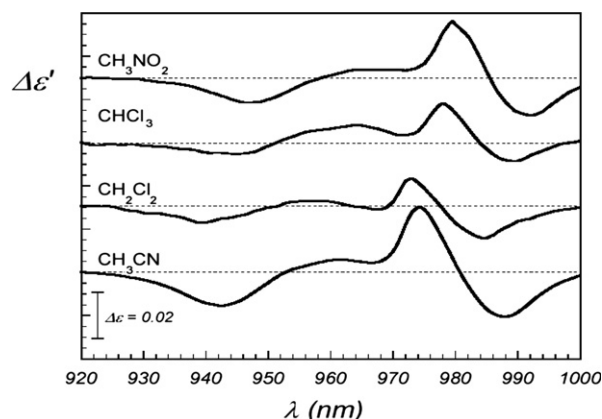
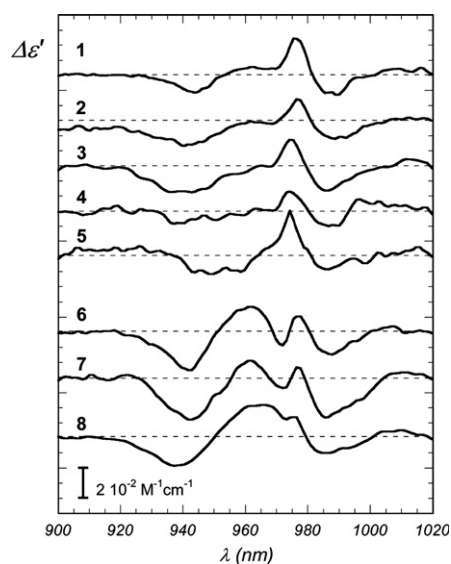


**Figure 1.** NIR CD spectra of YbX<sub>3</sub>/(*R,R*)-**1** mixtures in different solvents. In CH<sub>3</sub>CN and CH<sub>3</sub>NO<sub>2</sub> X<sup>−</sup> = TfO<sup>−</sup>, while in CHCl<sub>3</sub> and CH<sub>2</sub>Cl<sub>2</sub>, X<sup>−</sup> = Cl<sup>−</sup>. In all cases, the [YbX<sub>3</sub>]/[**1**] molar ratio was 1:4. The metal ion concentration [Yb<sup>3+</sup>] = 20 mM; Δε' is normalized to [Yb<sup>3+</sup>].

We noticed that the spectra do not show any time evolution: they appear as soon as one puts the cuvette in the spectropolarimeter, and stay indefinitely constant, at least on the hours/days timescale. Moreover, we could not detect any Cotton effect in mixtures of Yb(OTf)<sub>3</sub> with a very large excess of a chiral monofunctional alcohol: (*R*)-2-butanol (data not shown).

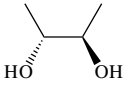
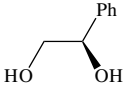
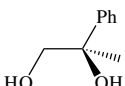
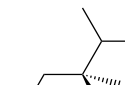
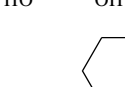
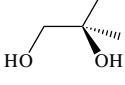
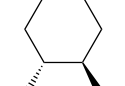
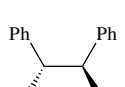
To investigate the behaviour with other diols, we focussed on acetonitrile and nitromethane as the solvents, since for (*R,R*)-2,3-butanediol, these choices lead to the strongest Cotton effects.

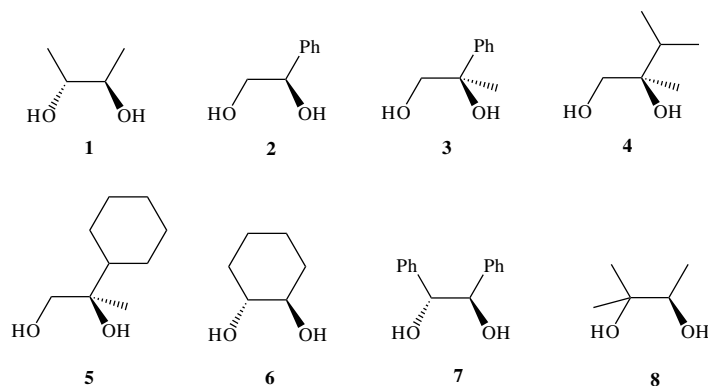
Figure 2 and Table 1 report the NIR CD spectra obtained in CH<sub>3</sub>CN on several diols with the same chirality (Scheme 1) (1:4 Yb/diol ratio, 20 mM Yb(OTf)<sub>3</sub>).



**Figure 2.** NIR CD spectra of the Yb/diol mixture with diols **1–8** (Yb/diol ratio 1:4, 0.5 mL, [Yb(TfO)<sub>3</sub>] = 20 mM in CH<sub>3</sub>CN, path length 1 cm, time constant 0.5 s, 50 nm/min); Δε' is normalized to [Yb<sup>3+</sup>]. From 4 to 32 scans were averaged. For a clearer comparison, the intensity of the spectra were multiplied by a scaling factor, as listed in Table 1.

**Table 1.** Scaling factors used in Figure 2, enantiomeric composition (ee), and intensity of the most intense Cotton effects for the NIR CD spectra of Figure 2

Entry	Diol	Scaling factor	Enantiomeric purity (ee (%))	$\Delta\epsilon'$ (940 nm) ( $10^{-3} \text{ M}^{-1} \text{ cm}^{-1}$ )	$\Delta\epsilon'$ (980 nm) ( $10^{-3} \text{ M}^{-1} \text{ cm}^{-1}$ )	$\Delta\epsilon'$ (990 nm) ( $10^{-3} \text{ M}^{-1} \text{ cm}^{-1}$ )
1		1	99	−11.3	24.1	−12.6
2		2	99	−7.9	7.1	−5.8
3		10	56	−1.7	1.7	−1.6
4		15	30	−0.5	0.7	−0.6
5		10	70	−1.1	2.5	−0.8
6		2	99	−12.5	5.3	−7.3
7		7	99	−4.0	1.0	−3.8
8		5	89	−3.7	2.8	−2.0

**Scheme 1.**

One can appreciate that, independent of the diol nature, NIR CD spectra look very similar.<sup>19</sup> The sign and wavelength of all the sizable Cotton Effects are substantially the same in all the cases examined. Minor differences are

mostly related to the band at 960 nm, while for diols **6–8**, this band is positive and the most intense one, for diol **1–5** its relative intensity is much lower and in some cases it becomes confused with noise.

These results show that there is at least one  $\text{Yb}^{3+}$ –diol adduct, of not yet determined stoichiometry. If two or more chiral ligand molecules are involved in determining the observed CD, it makes sense to investigate the behaviour of scalemic diol mixtures: in this case, the presence of the two enantiomers may lead to the formation of homochiral or heterochiral species, with different stability constants and each endowed with a different CD spectrum. As a consequence, one may observe linear or non-linear dependence of the CD amplitude on the enantiomeric composition. We acquired NIR CD spectra using (*R,R*)-2,3-butanediol with ee variable between 0% and 100%. Figure 3 reports the intensity of the main bands at 940, 980, 990 nm as a function of the diol ee. The linearity of the plot indicates that, within experimental error, the NIR CD spectrum is simply scaled by the effective ee, a result which will be discussed in the next section.

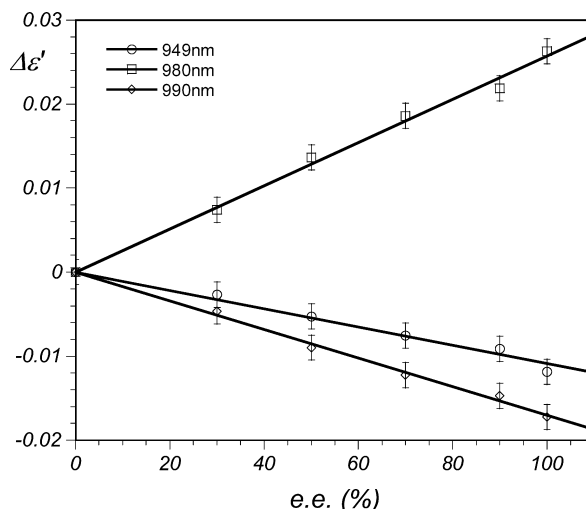


**Figure 3.** Plot of the NIR CD band intensities of the  $\text{Yb}(\text{TfO})_3/\mathbf{1}$  mixture as a function of the ee of **1**. The intensities are measured at 949, 980, 990 nm with a  $\text{Yb}/\text{diol}$  ratio 1:4;  $[\text{Yb}(\text{OTf})_3] = 5.25 \text{ mM}$  in  $\text{CH}_3\text{NO}_2$ , path length 10 cm,  $T = 298 \text{ K}$ ;  $\Delta\epsilon'$  is normalized to  $[\text{Yb}^{3+}]$ .

To gain insight into the stoichiometry of the dichroic complex, a full titration of  $\text{Yb}(\text{TfO})_3$  with diols **1** and **6** was performed. The titration with **1** was performed both in acetonitrile (Fig. 4A and B) and in nitromethane (Fig. 4C and D).

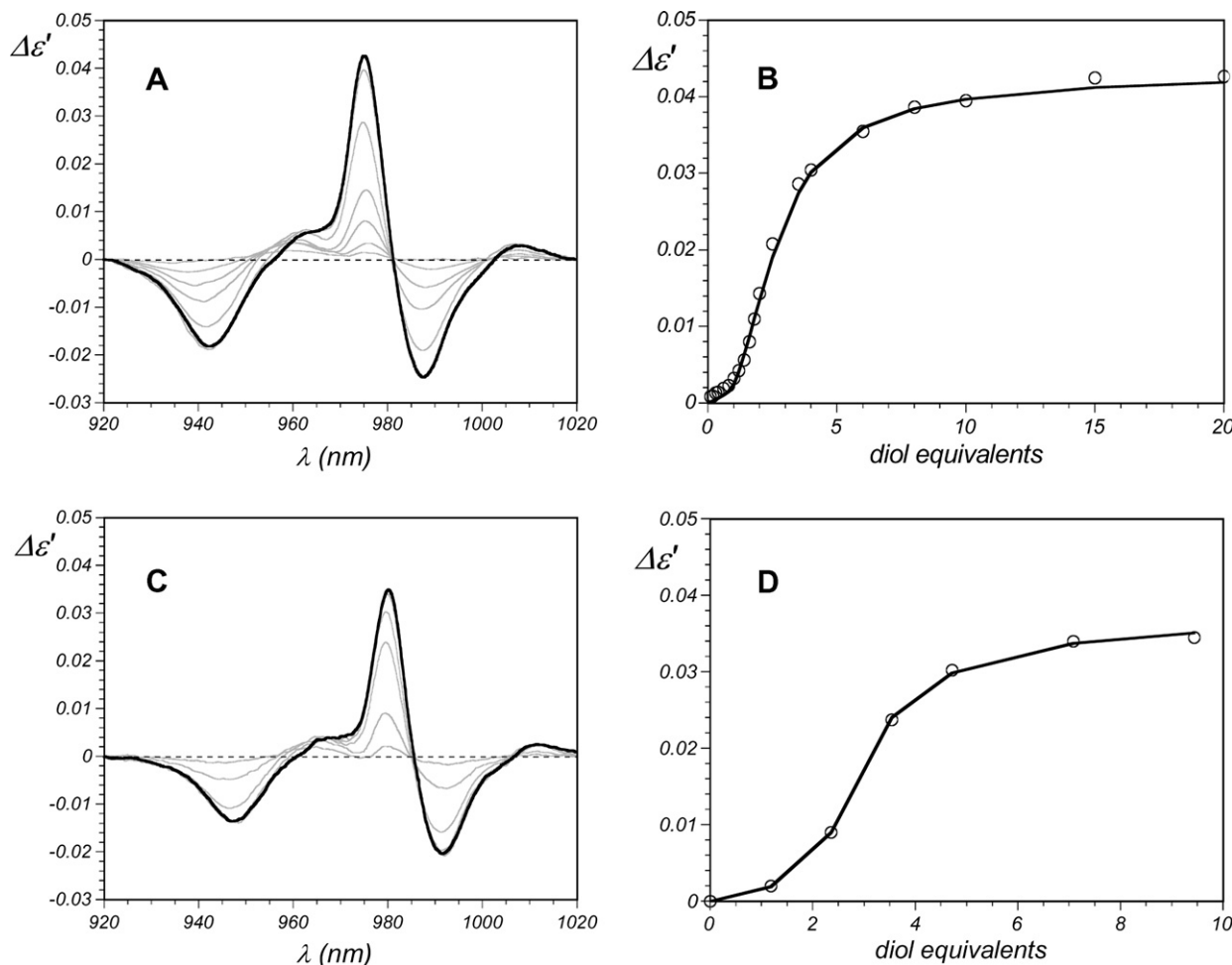


**Figure 4.** NIR CD titration of  $\text{Yb}(\text{OTf})_3$  with (*R,R*)-2,3-butane diol, **1**, in  $\text{CH}_3\text{CN}$  (A and B,  $[\text{Yb}(\text{TfO})_3] = 60 \text{ mM}$ ) and  $(\text{CH}_3\text{NO}_2)$  (C and D,  $[\text{Yb}(\text{TfO})_3] = 10 \text{ mM}$ );  $\Delta\epsilon'$  is normalized to  $[\text{Yb}^{3+}]$ . Plots (B) and (D) report the intensity of the maximum around 980 nm as a function of the diol equivalents; the dots indicate the experimental points and the continuous line is the result of the fitting, with the parameters of Table 2, as discussed in the text. For the sake of clarity (A) shows only the spectra at  $\rho = 0.4, 1.0, 1.6, 2.0, 3.5, 10.0$  (grey lines) and  $\rho = 20.0$  (dark line), and (C) shows only  $\rho = 1.18, 2.36, 3.54, 4.72, 7.08$  (grey lines) and  $\rho = 9.44$  (dark line).

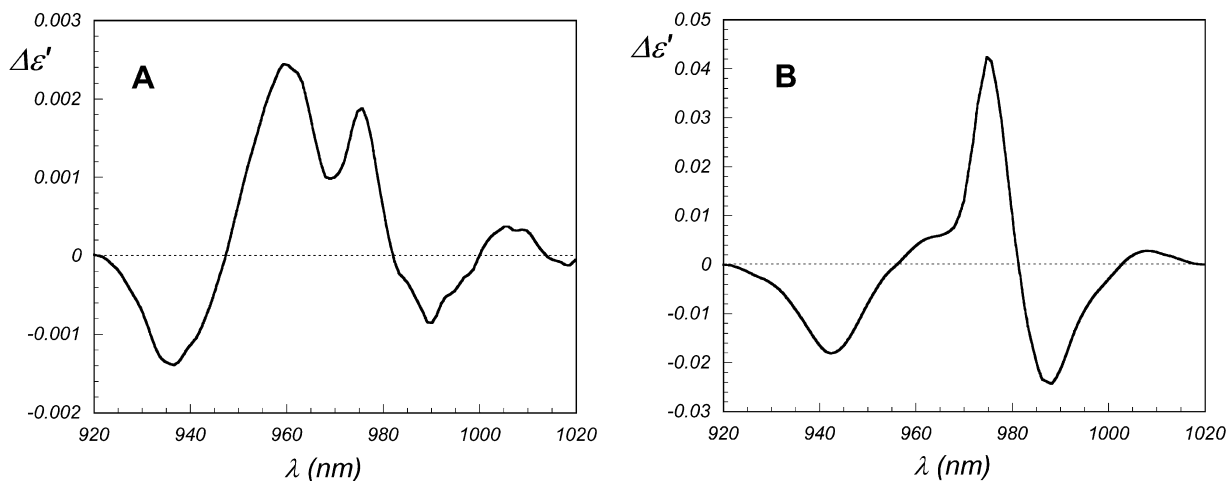


**Figure 5.** Profile of the NIR CD spectra at the beginning (A, 0.6 equiv of diol added) and the end of the titration (B, 20.0 diol equivalents) of  $\text{Yb}(\text{OTf})_3$  with **1** in  $\text{CH}_3\text{CN}$ . See Figure 4 for experimental conditions.

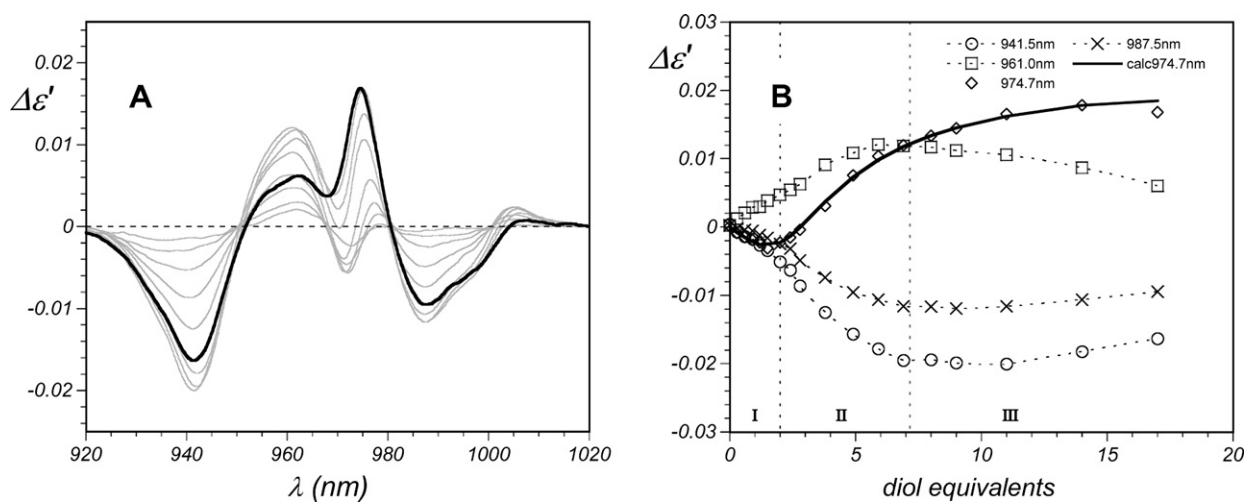


**Figure 6.** NIR CD titration of  $\text{Yb}(\text{OTf})_3$  with **6** in  $\text{CH}_3\text{CN}$  (A and B,  $[\text{Yb}(\text{TfO})_3] = 60 \text{ mM}$ );  $\Delta\epsilon'$  is normalized to  $[\text{Yb}^{3+}]$ . For the sake of clarity (A) shows only the spectra at  $\rho = 0.6, 1.2, 2.0, 2.8, 3.8, 5.9, 8.0, 11.0$  (grey line) and  $\rho = 17.0$  (dark line). In plot (B), the intensities at 941.5, 961.0, 974.7 and 987.5 nm are reported. The continuous line represents the results of the fitting at 975 nm, with the parameters of Table 2, as discussed below in the text. The dotted lines join the experimental points. The three important slope changes (I, II, III) are highlighted.

and D). After the first diol addition (equivalent to a diol-to-metal ratio  $\rho = 0.1$ ), a weak but detectable CD could be recorded. The binding constant is apparently higher in nitromethane than in acetonitrile: 7 diol equivalents are sufficient to reach completeness and fully titrate 10 mM of  $\text{Yb}(\text{TfO})_3$  in nitromethane, whereas up to 20 equiv are needed for a 60 mM solution in acetonitrile.

At low  $\rho$  values ( $\rho < 1$ ), the spectrum of  $\text{Yb}(\text{OTf})_3/\mathbf{1}$  takes the form shown in Figure 5A and only after an equimolar quantity of diol has been added, does it eventually convert to the final spectrum shown in Figure 5B. Apparently there are several different chiral chelates in solution whose relative proportion depends on the molar ratio between diol and metal. This is also evident in the s-shape of the Cotton effect

intensity around  $980 \text{ nm}^{\ddagger}$ ; the lack of an isosbestic point in the region around 960 nm confirms that the coexisting chiral species are more than two. It should be observed, however, that the positions and the signs of several relevant Cotton effects remain the same in the two complexes.

The titration with diol **6** in  $\text{CH}_3\text{CN}$  reveals again the consecutive formation of several diol-bound species (Fig. 6A and B): also the plot of the intensities at 941.5, 971,

<sup>‡</sup>We observed a small band shift on passing from  $\text{CH}_3\text{CN}$  to  $\text{CH}_3\text{NO}_2$ . The plots of Figure 4B and D were recorded at the wavelength of the maxima around 980 nm, corresponding to 974 nm and 979 nm, respectively.



**Table 2.** Formation constants and molar CD's obtained through non-linear fits of the titration curves in Figures 4B and D and 6B

Diol solvent	Yb(OTf) <sub>3</sub> /1		Yb(OTf) <sub>3</sub> /6
	CH <sub>3</sub> CN	CH <sub>3</sub> NO <sub>2</sub>	CH <sub>3</sub> CN
$K_1$ (mol/L) <sup>-1</sup>	~10 <sup>4</sup>	—	(1.4 ± 0.4)10 <sup>2</sup>
$K_2$ (mol/L) <sup>-1</sup>	(1.3 ± 0.4)10 <sup>2</sup>	—	(3.3 ± 0.9)10 <sup>1</sup>
$K_3$ (mol/L) <sup>-1</sup>	(1.5 ± 0.1)10 <sup>1</sup>	(1.9 ± 0.1)10 <sup>2</sup>	(7.1 ± 0.2)
$\Delta\epsilon_1$ (M <sup>-1</sup> cm <sup>-1</sup> )	~10 <sup>-3</sup>	—	(-2.7 ± 0.5)10 <sup>-3</sup>
$\Delta\epsilon_2$ (M <sup>-1</sup> cm <sup>-1</sup> )	(1.4 ± 0.1)10 <sup>-2</sup>	—	(-7.9 ± 0.5)10 <sup>-3</sup>
$\Delta\epsilon_3$ (M <sup>-1</sup> cm <sup>-1</sup> )	(4.4 ± 0.1)10 <sup>-2</sup>	(3.78 ± 0.05)10 <sup>-2</sup>	(2.34 ± 0.05)10 <sup>-2</sup>
$R^a$ (%)	2.8	1.3	3.1

The molar CD's  $\Delta\epsilon_1$ ,  $\Delta\epsilon_2$ ,  $\Delta\epsilon_3$ , are measured at 974 nm in CH<sub>3</sub>CN and 979 nm in CH<sub>3</sub>NO<sub>2</sub>. The constants  $K_1$ ,  $K_2$ ,  $\Delta\epsilon_1$ ,  $\Delta\epsilon_2$ , in CH<sub>3</sub>NO<sub>2</sub> could not be safely determined because of incomplete dissolution of Yb(OTf)<sub>3</sub>, and are not reported.

<sup>a</sup> The agreement factor  $R$  is defined as  $R = \sqrt{\frac{\sum_i (Y_i^{\text{exp}} - Y_i^{\text{calc}})^2}{\sum_i (Y_i^{\text{exp}})^2}}$ , where  $Y_i^{\text{exp}}$  and  $Y_i^{\text{calc}}$  are the experimental and calculated band intensity.

974.7, 987.5 nm indicate that at least three chiral complexes of different stoichiometries are progressively formed.

The numerical analysis of the NIR CD titration data for diols **1** and **6** through Eqs. 2–6 are reported in Table 2.

### 3. Discussion

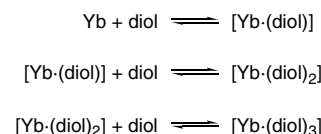
The collection of spectra in Figure 2 reveals how Yb–diol complexes are formed with a wide variety of molecules including a cyclic diol **6** and sterically hindered diols **7** and **8**. Polar solvents weakly coordinating lanthanides, such as nitromethane or even acetonitrile promote complex formation, by providing a suitable medium for the dissolution of the lanthanide salt and of the chiral ligand. It is noteworthy that the NIR CD spectrum of a mixture of diol **1** and Yb(OTf)<sub>3</sub> is weak but non-vanishing also in methanol as the solvent (data not shown), which clearly competes with the chiral ligand. The data reported so far in the literature indicate that Yb(III) NIR CD spectra depend primarily on the structure of the coordination polyhedron and to a lesser extent, if at all, on the ligand constitution.<sup>20,21</sup> On this basis, the analogies among the NIR CD spectra of diols **1–5** and **6–8** among the highest coordinated Yb/1 and Yb/6 species should be interpreted as complexes having a similar arrangement of the coordination polyhedron, and differences in the diol substituents have only a minor effect on the spectra.

In particular, when looking at the NIR CD spectra reported in Figure 2, we observed that there are some spectral features common between diols **6** and **8** (we shall define this NIR CD spectra *type A*) on one side and between **1** and **5** (*type B*) on the other. More specifically, *type A* and *type B* spectra differ in the magnitude of a positive band at 960 nm and a trough or a negative Cotton effect at 975 nm, which is apparent only for the *type A* set.

Upon closer inspection of the titration data of Figures 4 and 6, it can clearly be seen that several chiral species are formed. Figure 5 demonstrates that at a low diol-to-Yb molar ratio, diol **1** yields a *type A* spectrum, which eventually evolves into a *type B*. Similarly, at higher molar ratios, diol **6** provides a *type B* curve, as shown by the bold line of Figure 6. This suggests that the differences among *type A* and *type B* spectra are related to species with different stoi-

chiometry rather than to a different arrangement in the Yb–diol species.

We observed the formation of at least three different chiral complexes over the course of the titration of the Yb salt with both diols **1** and **6**, and we postulate the set of equilibria depicted in Scheme 2, where formally neutral species are considered purely for the sake of simplicity.

**Scheme 2.**

The identity of the NIR CD spectra in apolar solvents (Fig. 1) is the first indication that we should invoke on association with the counterion (TfO<sup>-</sup>) to form neutral ion pairs. Moreover, <sup>19</sup>F NMR spectra (not shown) of Yb(OTf)<sub>3</sub>/(*R,R*)-2,3-butanediol mixtures reveal that the tri-flate resonance is strongly shifted, witnessing its proximity to the paramagnetic centre. These considerations support the fact that the [Yb·(diol)<sub>3</sub>] species is the highest diol coordinate species in solution; the possible formation of a further diol coordinated [Yb·(diol)<sub>4</sub>] species appears quite unlikely (even if it cannot be completely excluded) in view of the crowded coordination sphere of the metal due to the four diol chelates and the participation of the counterion(s).

The numerical analyses of the titration curves, based on the equilibria of Scheme 2 and on the derived Eqs. 2–6 (see Section 5), fit very well the experimental data, as shown in Figures 4 and 6, with the parameters listed in Table 2, which also confirms that the equilibria of Scheme 2 are correct.

The binding constants fitted from the titration curves (Table 2) allowed us to reconstruct the spectra of the [Yb·(diol)<sub>3</sub>], and [Yb·(diol)<sub>2</sub>] species (Fig. 7). The [Yb·(diol)] species have a CD that is too weak to be safely reconstructed, hence they are not reported. It is apparent that the CD spectra of [Yb·(**1**)<sub>3</sub>] and [Yb·(**6**)<sub>3</sub>] look very similar, suggesting that the coordination polyhedra of these complexes are essentially identical. Since the conformation of the coordinating diol **6** is known, we deduce that also **1** binds the metal

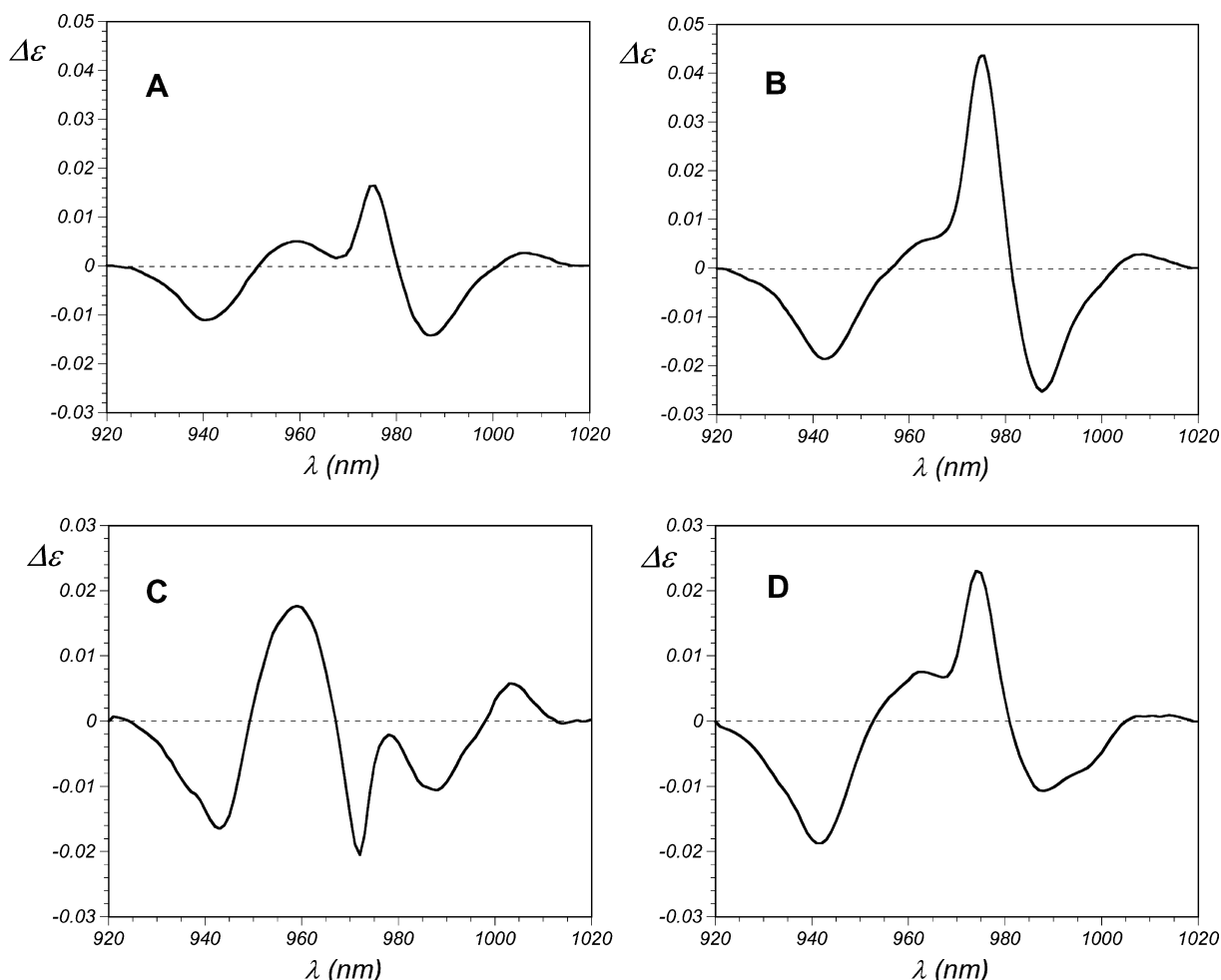


**Figure 7.** Reconstructed NIR CD spectra of the  $[\text{Yb}(\text{diol})_2]$  and  $[\text{Yb}(\text{diol})_3]$  species on the basis of the fitted binding constants (Table 2). (A) and (B) report the spectra of the  $[\text{Yb}(\mathbf{1})_2]$  and  $[\text{Yb}(\mathbf{1})_3]$  species, respectively. (C) and (D) the spectra of  $[\text{Yb}(\mathbf{6})_2]$  and  $[\text{Yb}(\mathbf{6})_3]$ , respectively.

in a  $g^-$  conformation, in strict analogy with what was observed in the diol coordination of  $[\text{Yb}(\text{fod})_3]$  complex.<sup>5,22</sup>

The binding constants are stronger for the less sterically hindered species **1** than for **6**, and their relative difference becomes larger for the more crowded tri-chelated species  $[\text{Yb}(\mathbf{1})_3]$  and  $[\text{Yb}(\mathbf{6})_3]$ . As previously observed, the formation constant in  $\text{CH}_3\text{NO}_2$  is larger than in  $\text{CH}_3\text{CN}$ , and we estimate here about one order of magnitude of difference.

The spectra of the di-chelated species  $[\text{Yb}(\mathbf{1})_2]$  and  $[\text{Yb}(\mathbf{6})_2]$  show differences, if they are compared with each other and if they are compared with the tri-chelated species. Differences are primarily related to the bands around 960 nm and a trough around 975 nm. This is not at all surprising considering that the coordination polyhedron is different with respect to tri-chelated species, and that structural differences among  $[\text{Yb}(\mathbf{1})_2]$  and  $[\text{Yb}(\mathbf{6})_2]$  are also possible: the larger steric hindrance of **6** may reflect in a different arrangement of the diol chelates as well as in a different participation of the counterions to the coordination.

Comparing these titrations, with the spectra of Figure 2, it is apparent that *type A* spectra must be associated with a stoichiometry  $[\text{Yb}(\text{diol})_2]$ , while *type B* with  $[\text{Yb}(\text{diol})_3]$

and that NIR CD immediately reveals which of the two systems is present. The differences among spectra **1–5** and **6–8** are probably related to smaller binding constants (mainly for the  $K_3$ ) in the sterically hindered species, and the correlation among the NIR CD spectra of  $[\text{Yb}(\mathbf{1})_3]$  and  $[\text{Yb}(\mathbf{6})_3]$  can be further extended to the other diols examined.

It is noteworthy that, in spite of the clear differences between *type A* and *B* NIR CD, there are at least three regions, around 940, 975 and 990 nm, which are invariably characterized by the same sign sequence (–, +, –) for diols of an (*R,R*)-configuration. This aspect and its implications will be further discussed in the following section.

The data of Figure 3 refer to a *type B* situation (the intensity ratio between the various bands reveal it), that is to a complex with formula  $[\text{Yb}(\mathbf{1})_3]$ . The linearity between the observed CD and the diol enantiomeric ratio should be noted. With this stoichiometry, starting from a scalemic mixture of **1**, one would expect the formation of the diastereomer  $[\text{Yb}((R,R)\text{-}\mathbf{1})_2((S,S)\text{-}\mathbf{1})]$ , which is chiral and should have an NIR CD completely different from  $[\text{Yb}((R,R)\text{-}\mathbf{1})_3]$ . On the contrary, we have no evidence of this process, which must be ruled out. Apparently, there is a complete stereo-

**Table 3.** Summary of the method of the Yb(OTf)<sub>3</sub>

Band	$\lambda$ (nm)	Sign ( <i>R,R</i> )- <i>sec-sec/sec-ter</i>	Sign ( <i>R</i> )- <i>prim-sec/prim-ter</i>
<b>I</b>	<b>940</b>	– ( <b>intense</b> )	– ( <b>intense</b> )
II	960	+ (intense)	+ (weak)
<b>III</b>	<b>976</b>	<b>+</b> ( <b>intense</b> )	<b>+</b> ( <b>intense</b> )
<b>IV</b>	<b>990</b>	– ( <b>intense</b> )	– ( <b>intense</b> )
V	1010	+ (weak)	+ (weak)

NIR CD spectra type  
for Yb(OTf)<sub>3</sub>/diol ratio 1:4



For each Cotton effect the sign for the (*R*)/(*R,R*) diol configuration for secondary and primary chiral diols is reported. The diagnostic bands are highlighted in bold.

selection, leading to the formation of homochiral adducts only. This is not completely new in the chemistry of chiral lanthanide chelates,<sup>18,23,24</sup> but is nonetheless interesting, especially with regards to the modest steric requirements of (*R,R*)-2,3,-butanediol as the ligand.

### 3.1. A new method for assigning the absolute configuration for chiral diols

The results presented above demonstrate that we have in our hands a new, easy and reliable method for assigning the absolute configuration of chiral diols. It consists of mixing an ytterbium salt (chloride or triflate) with a molar excess of the diol (not necessarily enantiopure), best in acetonitrile or nitromethane, and observing the NIR CD spectrum, which appears immediately after mixing and is indefinitely stable. A structured CD multiplet can be obtained, which permits a visual recognition of the similarity with the reference spectra.

As noted above, there are essentially two different situations, which we called *type A* and *B* spectra arising from complexes of formula [Yb·(diol)<sub>2</sub>] and [Yb·(diol)<sub>3</sub>], respectively. We know that at low molar ratios, a species [Yb·(diol)·(OTf)<sub>*n*</sub>]<sup>3–*n*</sup> exists, but is soon displaced in favour of the other two, when a larger amount of diol is added.

Both NIR CD spectra *type A* and *type B* are characterized by the sequence of signs (–, +, –) for the bands around 940, 976 and 990 nm for the diols presently investigated, all sharing the (*R*)/(*R,R*)-absolute configuration; we summarize in Table 3, the diagnostic bands of *type A* and *type B* spectra.

The steric requirements of the substituents on the chiral diol dictate a well-defined geometry of the coordination polyhedron, which gives rise to the observed NIR CD spectra. Unfortunately, the lack of a structural picture does not allow us to provide a deeper understanding of this relation, as we had reached in the case of Yb(fod)<sub>3</sub>.<sup>5</sup>

The perfect linearity with the enantiomeric excess featured in Figure 3 ensures that one can work with non-enantiopure samples. As final considerations on this method, it

should be noted that by working in a very shifted spectral region (near-IR), it does not suffer from spectroscopic interferences affecting other UV CD methods for the absolute configuration determination, which can often be attributed to chromophoric groups present in the analyte molecule; furthermore no particular purification of the diol, of the ytterbium salt or even of the solvent is needed, and that the method may tolerate the presence of alcohols or even water, as well as other common contaminants.

## 4. Conclusions

We have demonstrated the prompt formation of chiral complexes upon mixing a 1,2-diol with an ytterbium salt in a variety of solvents. These species give rise to easily detected NIR CD spectra, endowed with an easily recognizable fine structure. We connected the appearance of the CD multiplet to the complex stoichiometry, and we assigned the conformation of the binding diol. This study is a useful background and ensures a very simple tool to analyze diol/Yb mixtures, finding application, for example, in enantioselective reactions. One aspect, which may need further investigation, is that there were cases where the reaction product was itself an enantiomeric diol,<sup>25</sup> which may compete with the chiral auxiliary in binding Yb<sup>3+</sup> and participate in determining the reaction course.

The NIR CD spectrum lends itself to a novel method for determining the absolute configuration of chiral diols. This correlation is based purely on empirical grounds, but it offers a few positive advantages: the use of such a strongly red-shifted observation window allows one to investigate diols endowed with UV–vis absorbing group or even contaminants; the very structured NIR CD spectra aid visual recognition and testify that one deals with structurally related systems; water, which may be present in the Yb-salt, in the diol or in the solvent, does not prevent a successful measurement; we discussed in detail the cases of acetonitrile and nitromethane, but a wide variety of solvents can be used; scalemic diols can be analyzed; the chiral diol may be recovered through extraction.



## 5. Experimental

Enantiopure (*R,R*)- and (*S,S*)-2,3-butane diol **1**, and the diols **2** and **6** were purchased from Aldrich and Fluka, respectively and used without further purification (purity >98%; ee 99%). Diols **3**, **4**, **5**, **7**, **8** had been synthesized in our lab from the corresponding commercially available alkenes (Aldrich, Fluka) following Sharpless' procedure,<sup>1</sup> as reported in the literature.<sup>26</sup> The enantiomeric purities were checked by means of enantioselective HPLC and NMR. Commercial Yb(OTf)<sub>3</sub>, HPLC-grade acetonitrile and nitromethane were used (Fluka) without purification, as well as all the other solvents used to record the spectra of Figure 1. NIR CD spectra were recorded on a dedicated JASCO J-200 spectropolarimeter operating between 750 and 1350 nm, modified with a tandem Si/InGaAs detector with dual photomultiplier amplifier. For spectra recorded in CH<sub>3</sub>CN, a square quartz cell with 1.0 cm pathlength was used, with 3.2 nm bandwidth, 1.0 s and 0.5 s time constant, with scan speed 50 nm/min. For spectra recorded in CH<sub>3</sub>NO<sub>2</sub>, a 10.0 cm cell length was used with 3.2 nm bandwidth, 2.0 s time constant, with scan speed 20 nm/min, 8 scans for spectrum. <sup>19</sup>F NMR spectra were recorded on a Varian VXR 300 spectrometer operating at 7 T, after dissolving the sample in CD<sub>3</sub>CN (Amar, 99.8% atom D). For all the spectra (NIR CD and NMR) the temperature was 298 K.

### 5.1. Titration fitting

The mathematical expressions used to fit the experimental data in titrations of Figures 4 and 6 were derived considering the simultaneous actions of all the chemical equilibria described in the equations of Scheme 2. The three formation constants  $K_1$ ,  $K_2$ ,  $K_3$  were considered assuming unitary activity coefficients:

$$\frac{[\text{Yb(d)}]}{[\text{Yb}][\text{d}]} = K_1, \quad \frac{[\text{Yb(d)}_2]}{[\text{Yb(d)}][\text{d}]} = K_2, \quad \frac{[\text{Yb(d)}_3]}{[\text{Yb(d)}_2][\text{d}]} = K_3 \quad (1)$$

where [Yb(d)], [Yb(d)<sub>2</sub>], [Yb(d)<sub>3</sub>], [d], [Yb] are the concentrations of the mono-, di-, tris- diol-chelated species, the free diol **1** or **6**, and the free metal, respectively. From the combination of all these equilibria one obtains

$$[\text{d}]^4 + (K_3^{-1} + C(3-\alpha))[\text{d}]^3 + K_3^{-1}(K_2^{-1} + C(2-\alpha))[\text{d}]^2 + K_3^{-1}K_2^{-1}(K_1^{-1} + C(1-\alpha))[\text{d}] + K_3^{-1}K_2^{-1}K_1^{-1}C\alpha = 0 \quad (2)$$

and

$$[\text{Yb(d)}_3] = [\text{d}]^3 C / ([\text{d}]^3 + K_3^{-1}[\text{d}]^2 + K_3^{-1}K_2^{-1}[\text{d}] + K_3^{-1}K_2^{-1}K_1^{-1}) \quad (3)$$

$$[\text{Yb(d)}_2] = K_3^{-1}[\text{d}]^2 C / ([\text{d}]^3 + K_3^{-1}[\text{d}]^2 + K_3^{-1}K_2^{-1}[\text{d}] + K_3^{-1}K_2^{-1}K_1^{-1}) \quad (4)$$

$$[\text{Yb(d)}] = K_3^{-1}K_2^{-1}[\text{d}] C / ([\text{d}]^3 + K_3^{-1}[\text{d}]^2 + K_3^{-1}K_2^{-1}[\text{d}] + K_3^{-1}K_2^{-1}K_1^{-1}) \quad (5)$$

where  $C$  is the total metal concentration and  $\alpha$  are the equivalents of added diol. The numerical solution of Eq. 2 allows us to calculate the concentration of the single species through Eqs. 3–5. In turn, these are related to the observed CD intensity ( $\Delta A$ ) through

$$\Delta A = \Delta \epsilon_1[\text{Yb(d)}] + \Delta \epsilon_2[\text{Yb(d)}_2] + \Delta \epsilon_3[\text{Yb(d)}_3] \quad (6)$$

where  $\Delta \epsilon_1$ ,  $\Delta \epsilon_2$ ,  $\Delta \epsilon_3$  are the molar coefficients of the single chiral species. The set of simultaneous Eqs. 2–6 was included in a computer program (written in *Mathematica*<sup>27</sup> language) that optimizes the three binding constants  $K_1$ ,  $K_2$ ,  $K_3$  and the coefficients  $\Delta \epsilon_1$ ,  $\Delta \epsilon_2$ ,  $\Delta \epsilon_3$  in a least-square fitting of the experimental CD intensity ( $\Delta A$ ).

## Acknowledgement

Financial support from Ministero dell'Università e della Ricerca (Project FIRB RBPR05NWWC) is gratefully acknowledged.

## References

- Kolb, H. C.; Van Nieuwenhze, M. S.; Sharpless, K. B. *Chem. Rev.* **1994**, *94*, 2483.
- Salvadori, P.; Pini, D.; Petri, A. *Synlett* **1999**, 1181.
- Mlynarski, J.; Mitura, M. *Tetrahedron Lett.* **2004**, *45*, 7549–7552.
- Tsukube, H.; Shinoda, S. *Chem. Rev.* **2002**, *102*, 2389–2403.
- Di Bari, L.; Lelli, M.; Pintacuda, G.; Salvadori, P. *Chirality* **2002**, *14*, 265–273.
- Nakanishi, K.; Dillon, J. *J. Am. Chem. Soc.* **1971**, *93*, 4058–4060.
- Partridge, J. J.; Shiuey, S.; Chadha, N. K.; Baggiolini, E. G.; Blount, J. F.; Uskoković, M. R. *J. Am. Chem. Soc.* **1981**, *103*, 1253–1255.
- Tsukube, H.; Shinoda, S. *Enantiomer* **2000**, *5*, 13–22.
- Di Bari, L.; Salvadori, P. *Coord. Chem. Rev.* **2005**, *249*, 2854–2879.
- Richardson, F. *Inorg. Chem.* **1980**, *19*, 2806.
- Salvadori, P.; Rosini, C.; Bertucci, C. *J. Am. Chem. Soc.* **1984**, *106*, 2439.
- Di Bari, L.; Pintacuda, G.; Ripoli, S.; Salvadori, P. *Magn. Reson. Chem.* **2002**, *40*, 396–405.
- Ripoli, S.; Scarano, S.; Di Bari, L.; Salvadori, P. *Bioorg. Med. Chem.* **2005**, *13*, 5181–5188.
- Di Bari, L.; Pintacuda, G.; Salvadori, P. *J. Am. Chem. Soc.* **2000**, *122*, 5557–5562.
- Di Bari, L.; Lelli, M.; Pintacuda, G.; Pescitelli, G.; Marchetti, F.; Salvadori, P. *J. Am. Chem. Soc.* **2003**, *125*, 5549–5558.
- Lelli, M.; Pintacuda, G.; Cuzzola, A.; Di Bari, L. *Chirality* **2005**, *17*, 201–211.
- Lisowski, J.; Ripoli, S.; Di Bari, L. *Inorg. Chem.* **2004**, *43*, 1388–1394.
- Di Bari, L.; Lelli, M.; Salvadori, P. *Chem. Eur. J.* **2004**, *10*, 4594–4598.
- A large part of the intensity difference amongst the spectra is related to the enantiomeric purity of the diol used.
- Di Bari, L.; Pintacuda, G.; Salvadori, P.; Dickins, R. S.; Parker, D. *J. Am. Chem. Soc.* **2000**, *122*, 9257–9264.
- Dickins, R. S.; Parker, D.; Bruce, J. I.; Tozer, D. J. *J. Chem. Soc., Dalton Trans.* **2003**, 1264–1271.

22. Tsukube, H.; Hosokube, M.; Wada, M.; Shinoda, S.; Tamiaki, H. *Inorg. Chem.* **2001**, *40*, 740–745.
23. Aspinall, H. C.; Bickley, J. F.; Dwyer, J. L. m.; Greeves, N.; Kelly, R. V.; Steiner, A. *Organometallics* **2000**, *19*, 5416–5423.
24. Saá, J. M.; Tur, F.; González, J.; Vega, M. *Tetrahedron: Asymmetry* **2006**, *17*, 99–106.
25. Fukuzawa, S. I.; Yahara, Y.; Kamiyama, A.; Hara, M.; Kikuchi, S. *Org. Lett.* **2005**, *7*, 5809–5812.
26. Di Bari, L.; Pescitelli, G.; Pratelli, C.; Pini, D.; Salvadori, P. *J. Org. Chem.* **2001**, *66*, 4819–4825.
27. MATHEMATICA 5.0, Wolfram Research Inc. 2005, [www.wolfram.com](http://www.wolfram.com).